Processing Mixed-Mode GPS Networks for Deformation Monitoring Applications

Volker Janssen and Chris Rizos

Summary

The Global Positioning System (GPS) can be utilised in a wide range of deformation monitoring applications. During the past few years a methodology has been developed for processing data collected by GPS networks consisting of a mixed set of single-frequency and dual-frequency receivers. The strategy is to deploy a few permanent GPS stations with dual-frequency, geodetic-grade receivers surrounding an ›inner‹ network of low-cost, single-frequency GPS receivers. The dual-frequency GPS network is used to generate a file of ›corrections‹, analogous to Wide Area DGPS correction models for the distance dependent biases. These ›corrections‹ are then applied to the double-differenced phase observations from the inner receivers to improve baseline accuracy (primarily through empirical modelling of the residual atmospheric biases that otherwise would be neglected). The performance of this configuration has been investigated by simulating such a two-stage GPS network using data collected in different geographical regions.

Zusammenfassung

Das Global Positioning System (GPS) kann für eine ganze Reihe von Deformationsmessungen eingesetzt werden. In den letzten paar Jahren wurde eine Methode entwickelt, um Daten von GPS-Netzen auszuwerten, die sich aus einer gemischten Anzahl von Ein- und Zweifrequenzempfängern zusammensetzen. Die Strategie ist hierbei, ein inneres Netz von kostengünstigen Einfrequenzempfängern mit einigen, wenigen GPS-Referenzstationen von Zweifrequenzempfängern höchster Qualität zu umgeben. Das äußere Zweifrequenznetz wird benutzt, um eine Datei von ›Korrekturen‹ zu generieren (in Analogie zu Wide Area DGPS Korrekturmodellen für die distanzabhängigen Fehler). Diese ›Korrekturen‹ werden dann an die Doppeldifferenz-Phasenbeobachtungen der inneren Empfänger angebracht, um die Basisliniengenauigkeit zu verbessern (hauptsächlich durch empirische Modellierung der atmosphärischen Resteinflüsse, die sonst vernachlässigt werden würden). Die Leistungsfähigkeit dieser Konfiguration wurde untersucht, indem ein solches gemischtes GPS-Netz mit Daten aus verschiedenen geografischen Regionen simuliert wurde.

1 Introduction

The Global Positioning System (GPS) can be utilised in a wide range of deformation monitoring applications. The decreasing cost of GPS hardware, together with the increased reliability of the technology, facilitates such demanding applications as the monitoring of active volcanoes, tectonic fault lines, landslides, ground subsidence, bridges, dams, high-rise buildings, etc. GPS deformation measurements can be continuous, automatic, conducted in all weather conditions, and provide three-dimensional

positioning results. Higher computing power also means that the complex mathematics required to process GPS baselines can easily be handled in (near) real-time.

Deformation monitoring using GPS is usually carried out by installing and operating a local network of GPS receivers located on and around the deforming body. Numerous *continuous* GPS networks of different size have been established on tall buildings (Ogaja et al., 2001), bridges (Wong et al., 2001), dams (Behr et al., 1998), volcanoes (Owen et al., 2000), and on tectonic faults (Tsuji et al., 1995).

However, these networks are comparatively costly because they rely entirely on the use of dual-frequency instrumentation. In order to keep the cost of such a deformation monitoring system to a minimum, single-frequency GPS receivers need to be used. On the other hand, some atmospheric biases (mainly the ionospheric delay) cannot be accounted for directly if only one frequency is used. A single-frequency, carrier phase-tracking system is considered appropriate for small-scale continuous GPS networks if the baseline lengths are not longer than 10 km. This ›rule-of-thumb‹ implies that the differential ionospheric and tropospheric delay between the two receivers is essentially zero, and therefore does not impact on the baseline result. During solar sunspot cycle maximum periods, however, ionospheric disturbances have indeed corrupted L1 baseline measurements over distances less than 10 km, adversely affecting baseline repeatability (Janssen et al., 2001). It is therefore necessary to combine a single-frequency deformation monitoring network with a small number of dual-frequency receivers in order to account for these atmospheric effects. Such a *mixed-mode* configuration offers considerable flexibility and cost savings for deformation monitoring applications, which require a dense spatial coverage of GPS stations, and where it is not possible, nor appropriate, to establish permanent GPS networks using dual-frequency instrumentation. Hartinger/Brunner (2000) have used such a mixed-mode approach to monitor landslides in the Austrian Alps.

In this study a network of three dual-frequency GPS receivers surrounding the deformation zone is used to generate empirical ›correction terms‹ (Rizos et al., 2000). These double-differenced corrections are then applied to the data from the single-frequency baselines in the inner network to account for residual atmospheric biases. In this paper, the ionospheric correction model proposed for this mixed-mode system and the data processing strategy are described, and experimental results obtained in different geographical regions are presented.

2 Ionospheric Corrections

The ionosphere is a band of the Earth's upper atmosphere located approximately 50 km – 1000 km above the surface. The high spatial and temporal variability of the ionosphere has a major effect on GPS signals travelling from the satellite to the receiver. Moreover, the condition of the ionosphere is strongly related to the 11-year sunspot activity cycle. The most recent solar maximum occurred in 2000–2001, causing high ionospheric activity and having a clear impact on the results presented in this paper.

It is well known that the ionosphere is most active in a band extending up to about 20° on either side of the geomagnetic equator. This is also one of the two regions where small-scale ionospheric disturbances (short-term signal variations in amplitude and phase known as *scintillations*) mainly occur. The other being the high-latitude region close to the poles. In the equatorial region scintillations occur between approximately one hour after sunset until midnight (Klobuchar, 1996), and should have disappeared by 3 a.m. local time (IPS, 2002). The occurrence of scintillations also varies with the seasons. Between April and August they are less severe in the American, African and Indian longitude regions, while they are at a maximum in the Pacific region. The situation is reversed from September to March (Seeber, 1993). In mid-latitudes scintillations are rarely experienced, but Medium-Scale Travelling Ionospheric Disturbances (MSTIDs) occur frequently, mainly during daytime in the winter months, during periods of high solar activity, with a maximum around local noon (Wanninger, 1999).

While data from dual-frequency GPS receivers can account for the ionospheric delay directly by the appropriate linear combination of measurements made on both frequencies, data from single-frequency receivers cannot be corrected in this way. A simple ionosphere model transmitted within the navigation message can be used to account for about 50 % of the ionospheric range delay on L1 (Klobuchar, 1987). However, this is not sufficient for deformation monitoring applications where it is desired to detect movements of a few centimetres or less.

For deformation monitoring a *mixed-mode* GPS network approach can be adopted, where a fiducial network of dual-frequency receivers surrounding the deformation zone can be used to generate ›correction terms‹. These can then be applied to the single-frequency observations to account for the ionospheric effects and hence improve baseline accuracy. Figure 1 shows the ideal configuration of such a mixed-mode GPS network where the triangles denote fiducial stations, while the dots indicate single-frequency sites. The reference stations are to be situated outside the deformation zone but within the local tectonic region in order to avoid unwanted displacements of the external network.

Han/Rizos (1996) and Han (1997) have proposed a linear combination model which utilises a single ionospheric layer model at a height of 350 km. This approach can account for orbit bias and ionospheric delay, as well as mitigate tropospheric delay, multipath and measurement noise across the network. Data from the GPS re-

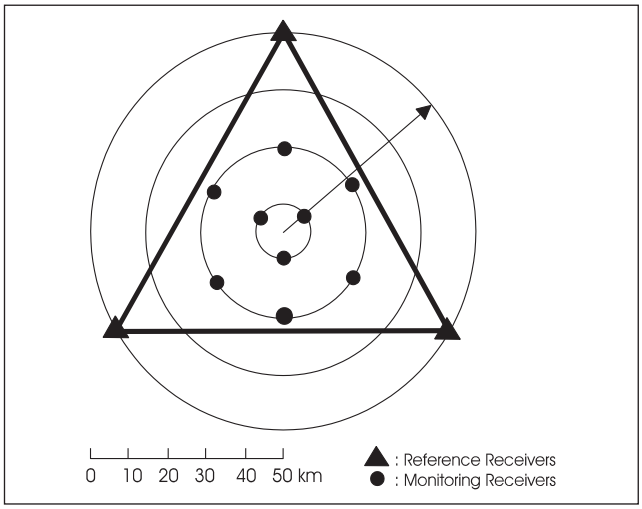

Fig. 1: Ideal network configuration of a mixed-mode GPS deformation monitoring network

ference station network can be used to derive empirical corrections to the double-differenced carrier phase data formed between the stations of the inner network.

2.1 Single-Differenced Model

The single-differenced carrier phase observation can be written as (Han, 1997):

$$\Delta\phi = \Delta\rho + \Delta d\rho - c\cdot\Delta dT + \lambda\cdot\Delta N - \Delta d_{ion} + \Delta d_{trop} + \Delta d^{\phi}_{mp} + \varepsilon_{\Delta\phi} \quad (1)$$

where Δ is the single-difference operator (difference between user and reference receiver), ϕ is the carrier phase observation in units of metres, ρ is the distance between receiver station and satellite, $d\rho$ is the effect of satellite ephemeris error on a particular receiver-satellite range, c is the speed of light, dT is the receiver clock error with respect to GPS time, λ is the wavelength of the carrier phase, N is the integer ambiguity for a particular satellite-receiver phase measurement, d_{ion} is the ionospheric delay, d_{trop} is the tropospheric delay, d^{ϕ}_{mp} is the carrier phase multipath effect, and $\varepsilon_{\Delta\phi}$ is the carrier phase observation noise in the one-way observation.

If more than one reference station is available, several single-differenced carrier phase observables can be obtained between the monitoring user receiver(s) and the reference receivers. In order to account for the distance dependent biases (orbit error, ionospheric delay and tropospheric delay) in equation (1), weights are introduced. These weights are inversely proportional to the baseline lengths and are used to average out the different distances between the user and the reference stations. Assuming a fiducial network consisting of three reference stations, a set of parameters α_i can be determined such that the following conditions are satisfied (Han/Rizos, 1996; Wu, 1994):

$$\sum_{i=1}^{3}\alpha_i = 1 \;,\; \sum_{i=1}^{3}\alpha_i\cdot\left(\vec{X}_u - \vec{X}_i\right) = 0 \quad \text{and} \quad \sum_{i=1}^{3}\alpha_i^2 = \min \quad (2)$$

where $\vec{X}_u$ and $\vec{X}_i$ are the user station position vector and reference station position vector in the Gaussian plane coordinate system respectively, while α_i denotes the weight for reference station i.

The linear combination of the single-differenced observables can now be written as:

$$\sum_{i=1}^{3}\alpha_i\cdot\Delta\phi_i = \sum_{i=1}^{3}\alpha_i\cdot\Delta\rho_i + \sum_{i=1}^{3}\alpha_i\cdot\Delta d\rho_i - c\cdot\sum_{i=1}^{3}\alpha_i\cdot\Delta dT_i + \lambda\cdot\sum_{i=1}^{3}\alpha_i\cdot\Delta N_i - \sum_{i=1}^{3}\alpha_i\cdot\Delta d_{ion,i} + \sum_{i=1}^{3}\alpha_i\cdot\Delta d_{trop,i} + \sum_{i=1}^{3}\alpha_i\cdot\Delta d^{\phi}_{mp,i} + \varepsilon_{\sum_{i=1}^{3}\alpha_i\Delta\phi_i} \quad (3)$$

According to the second condition in equation (2) the orbit bias term has been shown to be:

$$\sum_{i=1}^{3}\alpha_i\cdot\Delta d\rho_i \approx 0 \;. \quad (4)$$

Considering a user receiver u, the ionospheric delay can be expressed as:

$$\sum_{i=1}^{3}\alpha_i\cdot\Delta d_{ion,i} = d_{ion,u} - d_{ion,3} - \begin{bmatrix}\alpha_1 & \alpha_2\end{bmatrix}\cdot\begin{bmatrix} d_{ion,1} - d_{ion,3} \\ d_{ion,2} - d_{ion,3}\end{bmatrix} . \quad (5)$$

With increasing distance between the GPS reference stations the residual bias will become larger due to errors in the ionospheric delay interpolation.

If the tropospheric delay can be interpolated from the residual tropospheric delay at the reference stations, the tropospheric delay can be represented as:

$$\sum_{i=1}^{3}\alpha_i\cdot\Delta d_{trop,i} = d_{trop,u} - d_{trop,3} - \begin{bmatrix}x_u & y_u\end{bmatrix}\cdot\begin{bmatrix}x_1 & y_1 \\ x_2 & y_2\end{bmatrix}^{-1}\cdot\begin{bmatrix} d_{trop,1} - d_{trop,3} \\ d_{trop,2} - d_{trop,3}\end{bmatrix} \quad (6)$$

where (x_1, y_1), (x_2, y_2) and (x_u, y_u) are the coordinates of the reference and user receivers relative to reference station 3 in the Gaussian plane coordinate system. How close this term is to zero depends on the spatial correlation of the tropospheric delay. The residual tropospheric delay is largely influenced by the wet component of the troposphere, which is highly variable with height, time and geographic location making it very difficult to model. It can be expected that the tropospheric delay will be mitigated to some extent, but its effectiveness is an unknown function of the distance between the GPS receivers.

The carrier phase multipath effect can be expressed as:

$$\sum_{i=1}^{3}\alpha_i \cdot \Delta d^{\phi}_{mp,i} = d^{\phi}_{mp,u} - \sum_{i=1}^{3}\alpha_i \cdot d^{\phi}_{mp,i} \; . \qquad (7)$$

The second term on the right side of equation (7) is the weighted mean of the multipath values at the three reference receivers for this satellite. Due to the random nature of multipath at different receivers, this weighted mean will be reduced if all α_i ($i = 1, 2, 3$) are positive and less than 1, although the weight α_i is not derived from its standard deviation. On the other hand, the multipath at the user receiver will become a high-frequency bias, and will therefore be assumed to be close to random noise (Zhang/Schwarz, 1996). Hence it can be assumed that the multipath term has been significantly reduced and will consequently be ignored in the functional model.

The standard deviation of the one-way carrier phase observation can be approximated as a function of the elevation angle. If all GPS network receivers are located within a region of about 100 km radius, the elevation of a satellite is approximately the same. If σ^j denotes the approximated standard deviation of a one-way carrier phase observation, the standard deviation of the linear combination of single-differenced observations can be represented as:

$$\sigma_{\sum_{i=1}^{3}\alpha_i \cdot \Delta\phi_i} = \sqrt{1 + \alpha_1^{\,2} + \alpha_2^{\,2} + \alpha_3^{\,2}} \cdot \sigma^j \; . \qquad (8)$$

The single-differenced functional model can now be written in a simplified form:

$$\sum_{i=1}^{3}\alpha_i \cdot \Delta\phi_i = \sum_{i=1}^{3}\alpha_i \cdot \Delta\rho_i - c \cdot \sum_{i=1}^{3}\alpha_i \cdot \Delta dT_i + \lambda \cdot \sum_{i=1}^{3}\alpha_i \cdot \Delta N_i + \varepsilon_{\sum_{i=1}^{3}\alpha_i \cdot \Delta\phi_i} \; . \qquad (9)$$

2.2 Double-Differenced Model

Considering a user receiver u, equation (9) can be expressed as (Han, 1997):

$$\begin{aligned}\Delta\phi_{u,3} - \left[\alpha_1 \cdot \Delta\phi_{1,3} + \alpha_2 \cdot \Delta\phi_{2,3}\right] = {} & \Delta\rho_{u,3} - \left[\alpha_1 \cdot \Delta\rho_{1,3} + \alpha_2 \cdot \Delta\rho_{2,3}\right] \\ & - c \cdot \sum_{i=1}^{3}\alpha_i \cdot \Delta dT_i + \lambda \cdot \Delta N_{u,3} \\ & - \left[\alpha_1 \cdot \Delta N_{1,3} + \alpha_2 \cdot \Delta N_{2,3}\right] + \varepsilon_{\sum_{i=1}^{3}\alpha_i \cdot \Delta\phi_i} \; .\end{aligned} \qquad (10)$$

The double-differenced observation model can then be represented as:

$$\begin{aligned}\nabla\Delta\phi_{u,3} - \left[\alpha_1 \cdot \nabla\Delta\phi_{1,3} + \alpha_2 \cdot \nabla\Delta\phi_{2,3}\right] = {} & \nabla\Delta\rho_{u,3} \\ & - \left[\alpha_1 \cdot \nabla\Delta\rho_{1,3} + \alpha_2 \cdot \nabla\Delta\rho_{2,3}\right] + \lambda \cdot \nabla\Delta N_{u,3} \\ & - \left[\alpha_1 \cdot \nabla\Delta N_{1,3} + \alpha_2 \cdot \nabla\Delta N_{2,3}\right] + \varepsilon_{\sum_{i=1}^{3}\alpha_i \cdot \nabla\Delta\phi_i}\end{aligned} \qquad (11)$$

where $\nabla\Delta$ denotes the double-difference operator. Note that the receiver clock bias term cancels by forming the between-satellite differences.

Residual vectors can be formed from the double-differenced observations between reference stations 1 & 3 and 2 & 3:

$$V_{1,3} = \nabla\Delta\phi_{1,3} - \nabla\Delta N_{1,3} - \nabla\Delta\rho_{1,3} \qquad (12)$$

$$V_{2,3} = \nabla\Delta\phi_{2,3} - \nabla\Delta N_{2,3} - \nabla\Delta\rho_{2,3} \; . \qquad (13)$$

The double-differenced observable can then be written as:

$$\nabla\Delta\phi_{u,3} - \left[\alpha_1 \cdot V_{1,3} + \alpha_2 \cdot V_{2,3}\right] = \nabla\Delta\rho_{u,3} + \lambda \cdot \nabla\Delta N_{u,3} + \varepsilon_{\sum_{i=1}^{3}\alpha_i \cdot \nabla\Delta\phi_i} \; . \qquad (14)$$

After the initialisation of the reference stations the integer ambiguities are known, and together with the known coordinates, the correction vectors $V_{1,3}$ and $V_{2,3}$ can be determined. The ›correction term‹ $\left[\alpha_1 \cdot V_{1,3} + \alpha_2 \cdot V_{2,3}\right]$ can now be obtained and applied to the user receiver.

If the baseline between two GPS stations j and k of the inner network is considered, the linear combination can be written as:

$$\nabla\Delta\phi_{k,j} - \left[\alpha_1^{k,j} \cdot V_{1,3} + \alpha_2^{k,j} \cdot V_{2,3}\right] = \nabla\Delta\rho_{k,j} + \lambda \cdot \nabla\Delta N_{k,j} + \varepsilon_{k,j} \qquad (15)$$

where $\alpha_i^{k,j}$ is the difference in the α_i value for stations j and k, and $\left[\alpha_1^{k,j} \cdot V_{1,3} + \alpha_2^{k,j} \cdot V_{2,3}\right]$ is the ›correction term‹ for the inner baseline between these user receivers.

By forming the double-differenced observables between the inner single-frequency receivers, and using the residual vectors generated from the reference stations, the inner stations' coordinates can be determined without the need to use any GPS reference station observations at all. In practice, holding one reference site fixed, the baselines to the other two sites are processed and ›correction terms‹ are obtained for both baselines. These are then scaled (by means of the parameters α_i) according to the position of the inner stations inside the reference net-

work triangle to generate double-differenced corrections for the inner baselines.

The nature of these empirically-derived double-differenced ›correction terms‹ has been investigated by Janssen et al. (2001). A range of GPS data sets were processed incorporating a variety of baseline lengths, different geographical locations and different periods of sunspot activity (and hence ionospheric conditions). The standard deviation of the double-differenced ›correction terms‹ was found to be increasing linearly with increasing baseline length. The rate of increase was much more severe under solar maximum conditions as opposed to periods of low solar activity. This suggests that long baselines between reference stations might not be capable of generating reliable corrections under these conditions. However, the magnitudes of these biases are not entirely a function of distance, hence it is difficult to predict what should be the dimensions of the reference station network that would faithfully model the distance dependent biases. The geographic location of the network is certainly another contributing factor, as the ionospheric effects for GPS sites in the equatorial region are much larger compared to mid-latitude sites.

3 Single-Frequency Data Processing

A single-frequency version of the Baseline software package developed at UNSW is used to process the inner network incorporating the ›correction terms‹, which are determined using a modified version of the Bernese software. For deformation monitoring applications multi-baseline processing strategies should be used because all baselines are then computed together, taking into account the between-baseline correlations which arise from observing a GPS network simultaneously (Craymer/Beck, 1992). For continuous deformation monitoring a near real-time, epoch-by-epoch solution is desired in order to detect movements over a short period of time.

For a number of deformation monitoring applications, such as local networks around active volcanoes or dams, the deforming body itself will obstruct part of the sky. If the usual base-station/base-satellite approach is used in the GPS data processing, usually only the common satellites are considered. This results in the number of possible double-differences being comparatively low, hence a lot of potentially valuable information can be lost. As described in Janssen (2001), the Baseline software utilises a procedure to optimise the number of double-differenced observations used in the data processing. This method also considers satellites that are only visible from a small number of network stations. Hence, the number of independent double-differenced observables can be maximised in order to generate a more accurate and reliable solution. This data processing approach determines the receiver-to-satellite connections for each site of the network. A maximum set of independent double-differenced combinations is then computed using vector space methods and the geometric characterisations of Boolean matrices, as suggested by Saalfeld (1999).

4 Case Studies

4.1 Mid-Latitude Region

Data from the Southern California Integrated GPS Network (SCIGN) (SCIGN, 2002) were used to investigate the performance of the mixed-mode network configuration in the mid-latitude region. Figure 2 shows the location of the GPS sites, which are all equipped with dual-frequency receivers. The part of the network used in this study consists of an outer network of three sites (FXHS, FMTP, QHTP) surrounding an inner network of three sites (CSN1, OAT2, CMP9). The outer sites were used as fiducial GPS reference stations, indicated by triangles in Figure 2, while the inner sites (indicated by circles) simulated single-frequency receiver stations (by ignoring the observations made on L2). The data were collected under solar maximum conditions, using an observation rate of 30s, on three consecutive days from 8–10 August 2000 (DOY 221-223).

The fiducial baselines FXHS-FMTP and FXHS-QHTP are used to model the ionospheric conditions across the network. The L1 ›correction terms‹ for the inner baselines CSN1-OAT2 and CSN1-CMP9 can be determined by forming the linear combination according to equation (15) on a satellite-by-satellite and epoch-by-epoch basis.

As an example, Figure 3 shows the double-differenced corrections obtained for day 221. It can easily be recognised that ionospheric activity in mid-latitudes is mainly a daytime phenomenon. A comparison with directly generated ›correction terms‹ for the same baselines (using dual-frequency data) showed that the proposed pro-

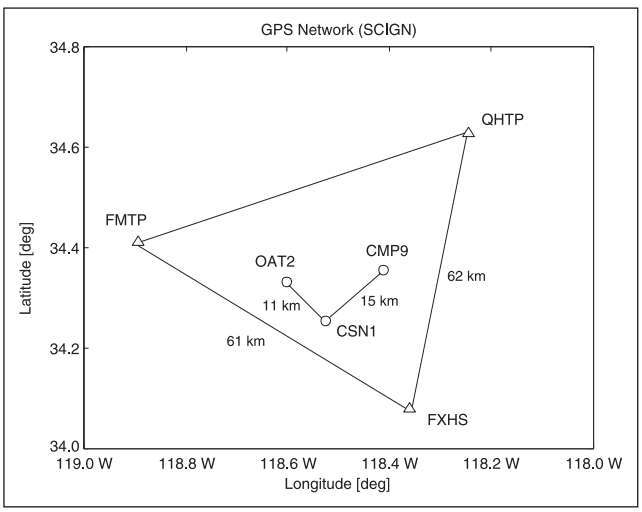

Fig. 2: SCIGN network stations used in this study

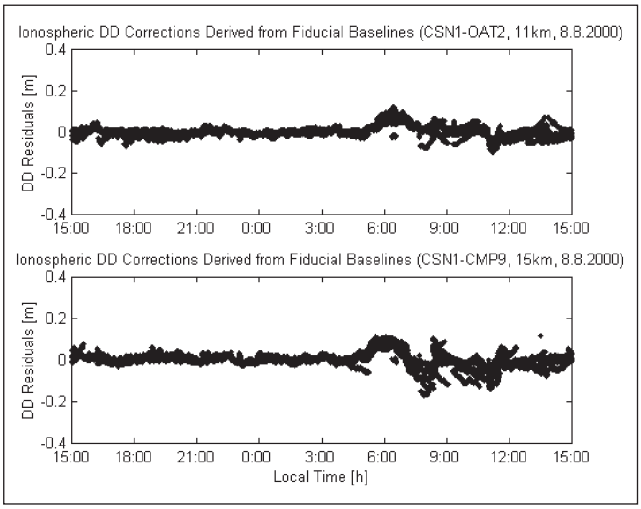

Fig. 3: Double-differenced L1 corrections for the inner baselines (DOY 221)

cedure does indeed compute correct values for the inner baselines.

The Baseline software is then used to process the inner baselines in single-frequency mode, with and without using the empirically-derived ionospheric ›correction terms‹. It can readily be assumed that no ground deformation has taken place during the time of observation. Hence, the baseline repeatability gives a good indication of the accuracy that can be achieved with the data processing strategy described in this paper. Figure 4 shows the results obtained for the inner baselines using the Baseline software without applying ionospheric corrections, while Figure 5 shows the results obtained by applying ionospheric corrections on day 221. The following days produce similar plots. The graphs show the Easting, Northing and Height components over a 24-hour period, each dot representing a single-epoch solution. In both

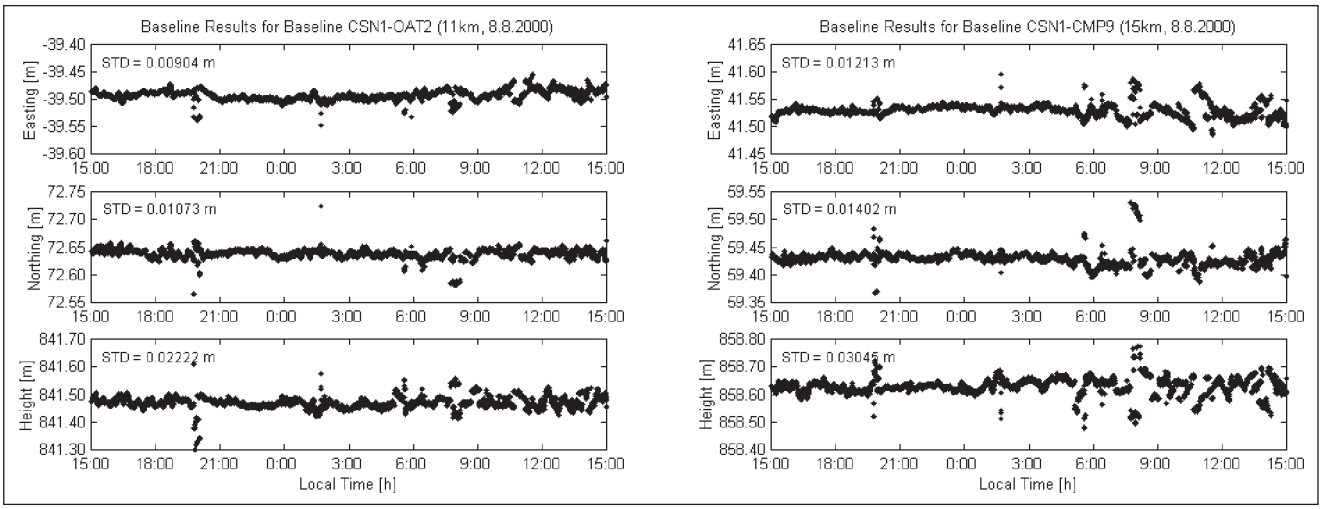

Fig. 4: Results for inner baselines not using ionospheric corrections (DOY 221)

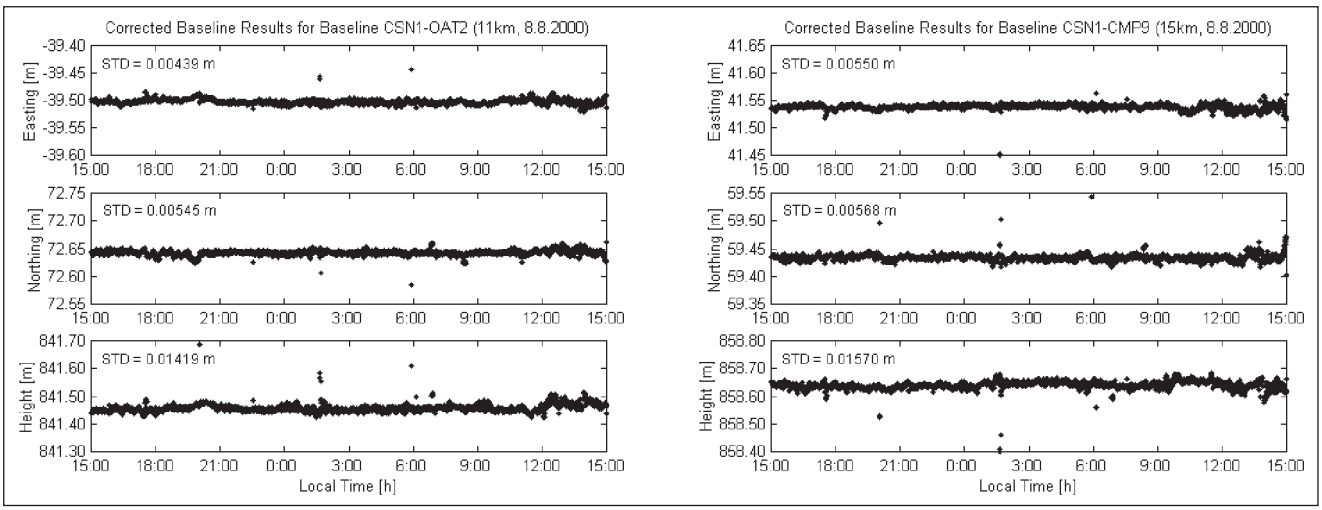

Fig. 5: Results for inner baselines applying ionospheric corrections (DOY 221)

	Day 221, no corr.	Day 221, corr.	Day 222, no corr.	Day 222, corr.	Day 223, no corr.	Day 223, corr.
Baseline CSN1-OAT2						
STD Easting [m]	0.00904	0.00439	0.00964	0.00597	0.01165	0.00538
STD Northing [m]	0.01073	0.00545	0.01114	0.00715	0.01415	0.00688
STD Height [m]	0.02222	0.01419	0.03241	0.01922	0.03513	0.02332
Baseline CSN1-CMP9						
STD Easting [m]	0.01213	0.00550	0.01401	0.00859	0.01709	0.00750
STD Northing [m]	0.01402	0.00568	0.01444	0.01024	0.02077	0.00916
STD Height [m]	0.03045	0.01570	0.03637	0.02438	0.04979	0.03280

Tab. 1: Standard deviations of the inner baseline components on days 221–223

Baseline	DOY	East [%]	North [%]	Height [%]
CSN1-	221	51.4	49.2	36.1
OAT2	222	38.1	35.8	40.7
(11 km)	223	53.8	51.4	33.6
CSN1-	221	54.7	59.5	48.4
CMP9	222	38.7	29.1	33.0
(15 km)	223	56.1	55.9	34.1
Average [%]		49	47	38

Tab. 2: Average improvement in the STD for both baselines on days 221–223

cases the Saastamoinen model was used to account for the tropospheric bias, as recommended by Mendes (1999).

Table 1 lists the standard deviations (STD) of the results obtained for the inner baselines using the two different processing strategies (not applying corrections versus applying corrections) on three successive days. Comparing Figures 4 and 5, and taking note of the information given in Table 1, it is evident that the baseline results are improved significantly by applying the ›correction terms‹. On average, the standard deviation of the baseline results has been reduced by almost 50 % in the horizontal and almost 40 % in the vertical component (Table 2). Using the proposed processing strategy, standard deviations of less than 1 cm horizontally and 1.5–3 cm vertically have been achieved for a single-epoch baseline solution (Table 1).

For baselines involving a significant difference in station altitude, as for example in GPS volcano deformation monitoring networks, the accuracy could be further improved by estimating an additional residual relative zenith delay parameter to account for the tropospheric bias. Among others, Abidin et al. (1998) claim that global troposphere models alone are not sufficient in such cases, and the relative tropospheric delay should be estimated.

4.2 Equatorial Region

Data from the Hong Kong GPS Active Network (Chen et al., 2001) were used to investigate the performance of the proposed network configuration in the low-latitude region. Figure 6 shows the location of the GPS sites, which are all equipped with dual-frequency receivers. The network consists of an outer network of three sites (HKKY, HKFN, HKSL) surrounding two inner sites (HKKT, HKLT). The outer sites were used as fiducial GPS reference stations, indicated by triangles in Figure 6, while the inner sites (indicated by circles) simulated single-frequency receiver stations (by ignoring the observations made on L2). Due to the absence of a third site within the fiducial triangle, the fiducial site HKKY was used to form the inner (single-frequency) baselines. Note that HKLT is located just outside the fiducial triangle, which should normally be avoided. However, this does not have any effect on the processing in this case, as HKKY-HKFN and HKKY-HKSL are used as fiducial baselines. The data were collected under solar maximum conditions, using an observation rate of 30s, on three consecutive days from 11–13 October 2000 (DOY 285-287).

According to equation (14) L1 ›correction terms‹ can be determined for the inner baselines HKKY-HKKT and HKKY-HKLT. As an example, Figure 7 shows the double-differenced corrections obtained for day 285. A comparison with directly generated ›correction terms‹ for the same baselines (using dual-frequency data) showed that

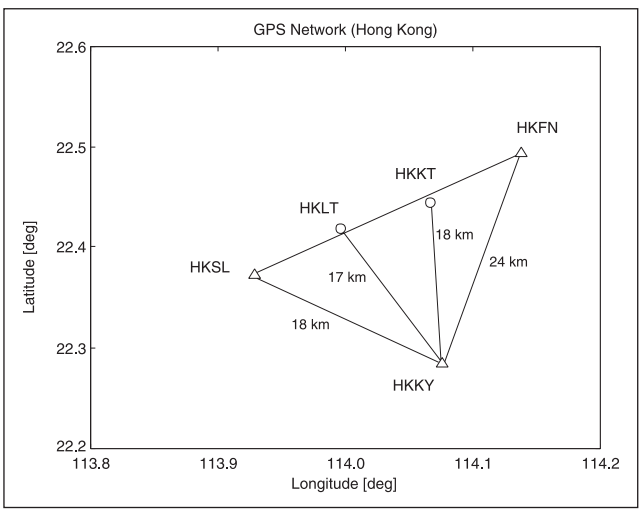

Fig. 6: Hong Kong GPS Active Network stations used in this study

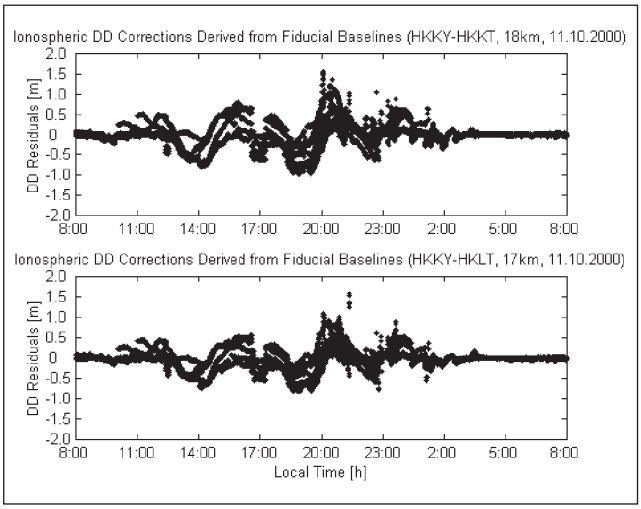

Fig. 7: Double-differenced L1 corrections for the inner baselines (DOY 285)

the proposed procedure does indeed compute correct values for the inner baselines.

It is evident that ionospheric activity in the equatorial region is much more severe than in mid-latitudes, reaching values of a few cycles. As expected, it mainly occurs after local sunset, although there is also a lot of daytime activity. This may be explained by intensified small-scale disturbances in the ionosphere during a period of increased solar activity. Furthermore, it can be identified as the primary diurnal maximum of the equatorial anomaly, also known as the *fountain effect* (high electron concentration observed on either side of the geomagnetic equator at magnetic latitudes of around 10–20°). Huang/Cheng (1991) state that the daily equatorial anomaly generally begins to develop at around 9–10 a.m. local time, reaching its primary maximum development at 2–3 p.m. local time. In periods of solar maximum condi-

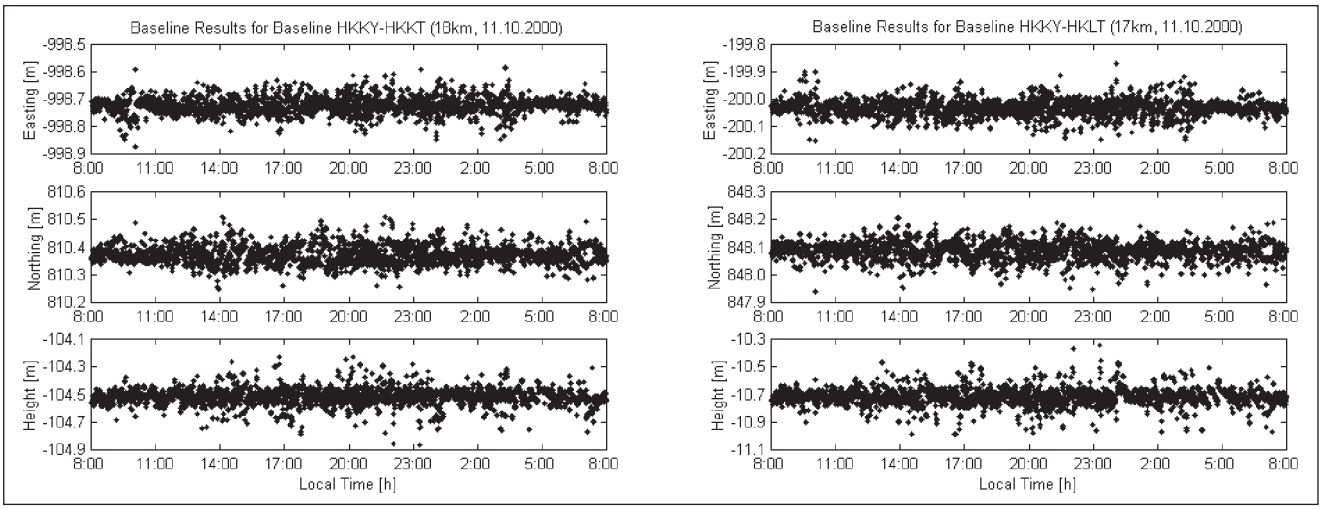

Fig. 8: Results for the inner baselines not using ionospheric corrections (DOY 285)

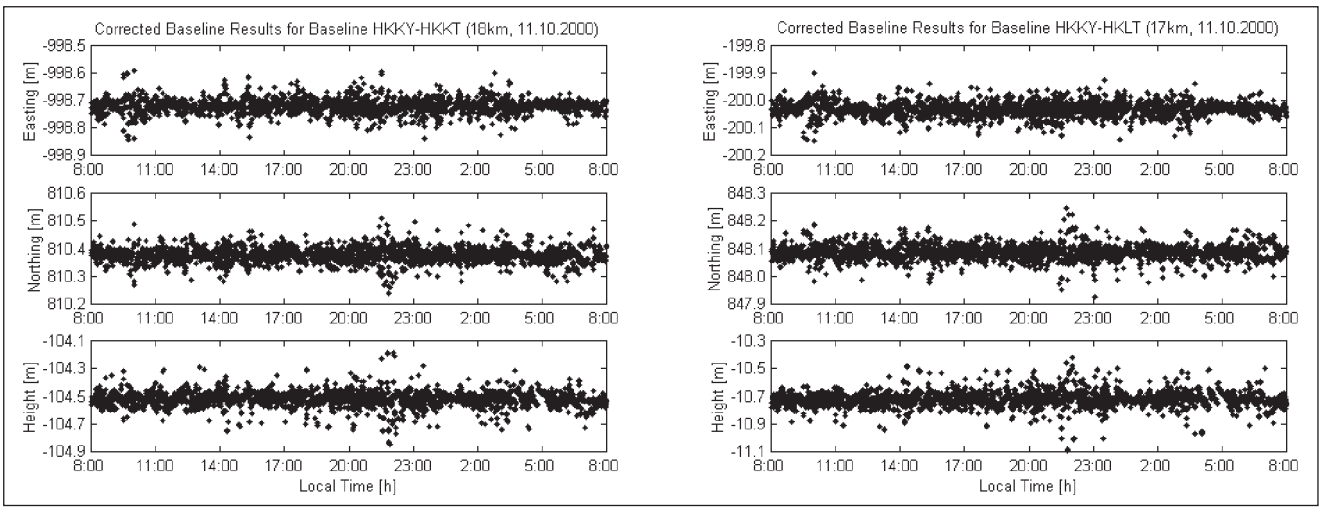

Fig. 9: Results for the inner baselines applying ionospheric corrections (DOY 285)

	Day 285, no corr.	Day 285, corr.	Day 286, no corr.	Day 286, corr.	Day 287, no corr.	Day 287, corr.
Baseline HKKY-HKKT						
STD Easting [m]	0.02994	0.02578	0.02888	0.02440	0.02738	0.02091
STD Northing [m]	0.03327	0.02635	0.03384	0.02814	0.02927	0.02197
STD Height [m]	0.06150	0.05774	0.06435	0.04770	0.06185	0.04519
Baseline HKKY-HKLT						
STD Easting [m]	0.02957	0.02508	0.02895	0.02452	0.02747	0.02049
STD Northing [m]	0.03265	0.02646	0.03579	0.03136	0.02991	0.02202
STD Height [m]	0.06204	0.05841	0.06526	0.05151	0.06208	0.04578

Tab. 3: Standard deviations of the inner baseline components on days 285–287

Baseline	DOY	East [%]	North [%]	Height [%]
HKKY-	285	13.9	20.8	6.1
HKKT	286	15.5	16.8	25.9
(18 km)	287	23.6	24.9	26.9
HKKY-	285	15.2	19.0	5.9
HKLT	286	15.3	12.4	21.1
(17 km)	287	25.4	26.4	26.3
Average [%]		18	20	19

Tab. 4: Average improvement in the STD for both baselines on days 285–287

tions, however, the anomaly is prone to peak after sunset, and gradients in the total electron content (TEC) are considerably larger at this secondary diurnal maximum (Skone, 2000).

Using the UNSW-developed Baseline software the inner baselines are processed in single-frequency mode, with and without using the empirically-derived ionospheric ›correction terms‹. It can be assumed that no ground deformation has taken place during the time of observation. Figure 8 shows the results obtained for the inner baselines using the Baseline software without applying ionospheric corrections, while Figure 9 shows the results obtained by applying ionospheric corrections on day 285. The following days produce similar plots. The graphs show the Easting, Northing and Height components over a 24-hour period on three successive days, each dot representing a single-epoch solution. As recommended by Mendes (1999), the Saastamoinen model was used to account for the tropospheric bias in both cases.

Table 3 lists the standard deviations (STD) of the results obtained for the inner baselines using the two different processing methods (not applying corrections versus applying corrections) on three successive days. Although it is not obvious from Figures 8 and 9, the baseline results are improved by applying the ›correction terms‹, as indicated in Table 3. On average, the standard deviation of the baseline results has been reduced by about 20 % in all three components (Table 4). The biggest improvement (of approximately 25 %) was achieved on day 287, the day with comparatively calm ionospheric conditions. This indicates that extreme ionospheric conditions, such as those experienced in close proximity to the geomagnetic equator during solar cycle maximum periods, can reduce the efficiency of the proposed method. This is most likely due to short-term effects of the highly variable ionosphere that cannot be modelled adequately. When applying the ›correction terms‹, the standard deviations still reach values of 2.0–3.5 cm in the horizontal components and 4.5–6.5 cm in the height component – values too large to permit reliable detection of ground deformation at the desired accuracy level.

Unfortunately, in spite of the shorter fiducial baseline lengths, the promising results obtained in the mid-latitudes could not be repeated for this network, situated in the equatorial region. This emphasizes the significant effect of the ionosphere on GPS deformation monitoring networks, especially at low-latitudes in periods of heightened solar activity.

5 Concluding Remarks

A procedure to process a mixed-mode GPS network for deformation monitoring applications has been described. Single-frequency GPS observations have been improved by generating empirical corrections obtained from a fiducial network of dual-frequency reference stations surrounding the inner single-frequency network. This method accounts for the ionospheric bias that otherwise would have been neglected when using single-frequency instrumentation only. Data from two GPS networks located in different geographical regions have been used to simulate such a network configuration in order to investigate the impact of the proposed processing strategy on baseline results.

The generated ›correction terms‹ have highlighted that the ionosphere has a significant effect on GPS baseline results. Even for short baselines this effect should not be neglected if it is desired to detect deformational signals with single-frequency instrumentation at a high accuracy.

In the mid-latitude region the single-frequency baseline repeatability has clearly been improved by applying

the empirical ›correction terms‹. The standard deviation of the baseline results has been reduced by almost 50 % in the horizontal and almost 40 % in the vertical component. Standard deviations of less than 1 cm horizontally and 1.5–3 cm vertically have been achieved for a single-epoch baseline solution.

In the equatorial region an improvement of approximately 20 % in all three components has been achieved by applying the corrections. However, the findings also indicate that extreme ionospheric conditions, such as those experienced in close proximity to the geomagnetic equator during solar cycle maximum periods, can reduce the efficiency of the proposed method. The standard deviation of the baseline components for a single-epoch baseline solution could not be reduced below about 2.0–3.5 cm horizontally and 4.5–6.5 cm vertically – values too large to permit deformation monitoring at the desired accuracy level. Nevertheless, the approach of processing a mixed-mode GPS network described in this paper can be a cost-effective and accurate tool for deformation monitoring suitable for a variety of applications.

Acknowledgements

SCIGN and its sponsors, as well as A/Prof. Peter Morgan from the University of Canberra, are thanked for providing the data used in this study. The first author is supported by an International Postgraduate Research Scholarship (IPRS) and funding from the Australian Research Council (ARC). The DVW is gratefully acknowledged for providing travel support for the first author to undertake his Ph.D. studies in Sydney, Australia.

References

Abidin, H. Z., Meilano, I., Suganda, O. K., Kusuma, M. A., Muhardi, D., Yolanda, O., Setyadji, B., Sukhyar, R., Kahar, J. and Tanaka, T.: Monitoring the Deformation of Guntur Volcano Using Repeated GPS Survey Method. Proc. 11th FIG Int. Congress, Commission 5, Brighton, UK, 19–25 July, 153–169, 1998.

Behr, J. A., Hudnut, K. W. and King, N. E.: Monitoring Structural Deformation at Pacoima Dam, California, Using Continuous GPS. Proc. ION GPS-98, Nashville, Tennessee, 15–18 September, 59–68, 1998.

Chen, W., Hu, C., Chen, Y., Ding, X. and Kwok, S. C. W.: Rapid Static and Kinematic Positioning with Hong Kong GPS Active Network. Proc. ION GPS-2001, Salt Lake City, Utah, 11–14 September, 346–352, 2001.

Craymer, M. R. and Beck, N.: Session Versus Single-Baseline GPS Processing. Proc. ION GPS-92, Albuquerque, New Mexico, 16–18 September, 995–1004, 1992.

Han, S.: Carrier Phase-Based Long-Range GPS Kinematic Positioning. PhD Dissertation, UNISURV S-49, School of Geomatic Engineering, The University of New South Wales, Sydney, Australia, 1997.

Han, S. and Rizos, C.: GPS Network Design and Error Mitigation for Real-Time Continuous Array Monitoring Systems. Proc. ION GPS-96, Kansas City, Missouri, 17–20 September, 1827–1836, 1996.

Hartinger, H. and Brunner, F. K.: Development of a Monitoring System of Landslide Motions Using GPS. Proc. 9th FIG Int. Symp. on Deformation Measurements, Olsztyn, Poland, Sep 1999, 29–38, 2000.

Huang, Y.-N. and Cheng, K.: Ionospheric Disturbances at the Equatorial Anomaly Crest Region during the March 1989 Magnatic Storms. Journal of Geophysical Research 96(A8): 13953–13965, 1991.

IPS: Space Weather and Satellite Communications. Fact sheet, http://www.ips.gov.au/papers/richard/space_weather_satellite_communications.html, 2002.

Janssen, V.: Optimizing the Number of Double-Differenced Observations for GPS Networks in Support of Deformation Monitoring Applications. GPS Solutions 4(3): 41–46, 2001.

Janssen, V., Roberts, C., Rizos, C. and Abidin, H. Z.: Experiences with a Mixed-Mode GPS-Based Volcano Monitoring System at Mt. Papandayan, Indonesia. Geomatics Research Australasia 74: 43–58, 2001.

Klobuchar, J. A.: Ionospheric Time-Delay Algorithm for Single-Frequency GPS Users. IEEE Transactions on Aerospace and Electronic Systems AES-23(3): 325–331, 1987.

Klobuchar, J. A.: Ionospheric Effects on GPS. In: Parkinson, B. W. and Spilker, J.J. (Eds.), Global Positioning System: Theory and Applications Volume I. Progress in Astronautics and Aeronautics, 163, American Inst. of Aeronautics and Astronautics, Washington, 485–515, 1996.

Mendes, V. B.: Modeling the Neutral-Atmosphere Propagation Delay in Radiometric Space Techniques. PhD Dissertation, Dept. of Geodesy & Geomatics Eng. Tech. Rept. No. 199, University of New Brunswick, Fredericton, Canada, 1999.

Ogaja, C., Rizos, C., Wang, J. and Brownjohn, J.: A Dynamic GPS System for On-line Structural Monitoring. Int. Symp. on Kinematic Systems in Geodesy, Geomatics & Navigation (KIS 2001), Banff, Canada, 5–8 June, 290–297, 2001.

Owen, S., Segall, P., Lisowski, M., Miklius, A., Murray, M., Bevis, M. and Foster, J.: January 30, 1997 Eruptive Event on Kilauea Volcano, Hawaii, as Monitored by Continuous GPS. Geophysical Research Letters 27(17): 2757–2760, 2000.

Rizos, C., Han, S., Ge, L., Chen, H. Y., Hatanaka, Y. and Abe, K.: Low-Cost Densification of Permanent GPS Networks for Natural Hazard Mitigation: First Tests on GSI's GEONET Network. Earth, Planets & Space 52(10): 867–871, 2000.

Saalfeld, A.: Generating Basis Sets of Double Differences. Journal of Geodesy 73: 291–297, 1999.

SCIGN: Southern California Integrated GPS Network (SCIGN) website: http://www.scign.org/, 2002.

Seeber, G.: Satellite Geodesy. De Gruyter, Berlin, Germany, 1993.

Skone, S. H.: Wide Area Ionosphere Modeling at Low Latitudes – Specifications and Limitations. Proc. ION GPS-2000, Salt Lake City, Utah, 19–22 September, 643–652, 2000.

Tsuji, H., Hatanaka, Y., Sagiya, T. and Hashimoto, M.: Coseismic Crustal Deformation from the 1994 Hokkaido-Toho-Oki Earthquake Monitored by a Nationwide Continuous GPS Array in Japan. Geophysical Research Letters 22(13): 1669–1672, 1995.

Wanninger, L.: The Performance of Virtual Reference Stations in Active Geodetic GPS-Networks under Solar Maximum Conditions. Proc. ION GPS-99, Nashville, Tennessee, 14–17 September, 1419–1427, 1999.

Wong, K.-Y., Man, K.-L. and Chan, W.-Y.: Monitoring Hong Kong's Bridges – Real-Time Kinematic Spans the Gap. GPS World 12(7): 10–18, 2001.

Wu, J. T.: Weighted Differential GPS Method for Reducing Ephemeris Error. Manuscripta Geodaetica 20: 1–7, 1994.

Zhang, Q. J. and Schwarz, K. P.: Estimating Double Difference GPS Multipath under Kinematic Conditions, Proc. IEEE Position Location & Navigation Symp. (PLANS '96), Atlanta, Georgia, 22–26 April, 285–291, 1996.

Authors' address

Dipl.-Ing. Volker Janssen and Prof. Chris Rizos
School of Surveying and Spatial Information Systems
The University of New South Wales
Sydney NSW 2052
Australia
v.janssen@student.unsw.edu.au, c.rizos@unsw.edu.au
www.gmat.unsw.edu.au/snap/